JOURNAL OF SOLID STATE CHEMISTRY 120, 254–259 (1995)

$CuNd_2Ge_2O_8$: Crystal Growth, Crystal Structure, and Magnetic and Spectroscopic Properties[1]

J. A. Campá

Facultad de Ciencias Geológicas, UCM, 28040 Madrid, Spain

E. Gutiérrez-Puebla, M. A. Monge, and C. Ruíz Valero

Instituto de Ciencia de Materiales, CSIC, Serrano 113, 28006 Madrid, Spain; and Laboratorio de Difracción de Rayos X y Cristalografía, Facultad de Ciencias Químicas, UCM, 28040 Madrid, Spain

J. Mira and J. Rivas

Departamento de Física Aplicada, Facultad de Física, Universidad de Santiago de Compostela, 15706 Santiago de Compostela, Spain

and

C. Cascales and I. Rasines[2]

Instituto de Ciencia de Materiales, CSIC, Serrano 113, 28006 Madrid, Spain

Received April 18, 1995; in revised form July 10, 1995; accepted July 13, 1995

After crystals of $CuNd_2Ge_2O_8$ are grown using CuO as self flux, the crystal structure is determined by single-crystal X-ray diffraction in the space group *Cm* (No. 8) to an *R* value of 5.1%. It is monoclinic, with $a = 9.846(2)$Å, $b = 15.335(5)$ Å, $c = 8.336(1)$ Å, $\beta = 148.48(2)°$, $V = 657.9(5)$ Å^3, $Z = 4$, and $D_c = 6.31$ g cm^{-3}. $CuNd_2Ge_2O_8$ shows a novel tridimensional structure type with chains of very distorted CuO_6 octahedra, two kinds of coordinations for germanium (GeO_5 trigonal bipyramids and rather regular GeO_4 tetrahedra), and NdO_8 triangulated dodecahedra. Above 100 K the reciprocal of the dc magnetic susceptibility of $CuNd_2Ge_2O_8$ follows the Curie–Weiss law $\chi^{-1} = 162(1)T + 5971(93)$ g Oe/emu, with a Weiss constant of $\theta = 36.8(7)$ K and a correlation factor $R = 0.99997$. Infrared spectra in the range 1000–100 cm^{-1} are related to those of comparable species. The absorption spectrum at room temperature in the 350–700 nm region is also given.

[1] See NAPS Document 05250 for 8 pages of supplementary material. Order from ASIS/NAPS, Microfiche Publications, P.O. Box 3513, Grand Central Station, New York, NY 10163. Remit in advance $4.00 for microfiche copy or for photocopy, $7.75 for up to 20 pages plus $0.30 for each additional page. All orders must be prepaid. Institutions and organizations may order by purchase order. However, there is a billing and handling charge for this service of $15.00. Foreign orders add $4.50 for postage and handling, for the first 20 pages, $1.00 for each additional 10 pages of material, and $1.50 for postage of any microfiche orders.

[2] To whom correspondence should be addressed.

I. INTRODUCTION

The combination of 3*d* transition metals, *T*, and rare earths, *R*, gives rise to a large number of *T*–*R* compounds: either binary *T*–*R* intermetallics, or species like *T*–*R* borides, carbides, nitrides, and oxides among others, in which both metals can be thought of as embedded into a matrix formed by atoms or anions of various *p* elements. Because of their interesting physical properties a good number of *T*–*R* compounds have recently raised a high degree of attention. At present some of them find applications as superconductors, as piezoelectric materials or permanent magnets, in magneto-optical recording, or as lasers. The authors have been recently aware of the lack of available information on germanates containing copper and a rare earth. As far as we know, none of these compounds have been prepared in the form of single crystals. For this reason we have tried to grow crystals of Cu–*R* germanates, in order to determine their crystal structure and some of their physical properties. This paper includes the results that we have obtained for $CuNd_2Ge_2O_8$.

II. EXPERIMENTAL DETAILS

Crystal growth. A good number of our attempts at growing crystals of the title compound showed that the method to grow such crystals has to take into account the high viscosity of the melts containing GeO_2. In conse-

0022-4596/95 $12.00

quence, nominal compositions near $CuR_2Ge_2O_8$ have to be avoided because they lead to a massive nucleation and to agglomerates of microcrystals showing an aplitic structure. Mixtures with relatively high contents of CuO acting as self flux give single crystals of several millimeters in size. Crystals of $CuNd_2Ge_2O_8$ used for this work were grown from mixtures of reagent-grade CuO, Nd_2O_3, and GeO_2 at molar ratios Cu:Nd:Ge = 4:1:3 in platinum crucibles. These mixtures were heated to 1260°C, soaked for 30 min, cooled to 1000°C at the rate of 4°C h^{-1}, and subsequently cooled to room temperature after turning the power off. After completely removing the excess of flux with dilute nitric acid, the resulting mass was filtered, dried, and identified as a mixture of $CuNd_2Ge_2O_8$ single-crystals, with some crystals of CuO and $CuGeO_3$. All these crystals were characterized by energy dispersive X-ray analysis and X-ray powder diffraction as indicated elsewhere (1). Crystals identified (2, 3) as $CuNd_2Ge_2O_8$ could be isolated using 30% HCl, which dissolves CuO and $CuGeO_3$ and does not attack $CuNd_2Ge_2O_8$ crystals.

Magnetic measurements. SQUID (Quantum Design) and Vibrating Sample (DMS-1660) magnetometers, operating from 300 to 4 K under zero-field cooling conditions at various fields between 0 and 1000 Oe were used to perform the dc magnetic measurements in single crystals of $CuNd_2Ge_2O_8$ and a polycrystalline sample of $CuY_2Ge_2O_8$. Diamagnetic corrections (4) for magnetic susceptibilities were taken into account. The polycrystalline sample of $CuY_2Ge_2O_8$ was prepared by heating stoichiometric amounts of reagent-grade CuO, Y_2O_3, and GeO_2 to 925°C during 1 week.

Spectroscopic studies. A FT-IR Nicolet SX60 spectrometer was used in the range 4000–100 cm^{-1} with powdered samples dispersed either in KBr or in polyethylene pellets. The absorption spectrum was recorded at room temperature in the wavelength region between 350 and 700 nm using a Kontron Uvikon 820 spectrophotometer. The lower limit corresponds to the absorption edge of the matrix. At higher energies the strong matrix absorption overlapped with the $4f$–$4f$ transitions of the Nd^{3+}, preventing the observation of the high-energy part of the spectrum.

X-ray structure determinations. A blue crystal showing well defined faces was mounted in a kappa diffractometer. A summary of its fundamental data is given in Table 1. The cell dimensions were refined by least-squares fitting the θ values of 25 reflections. The intensities were corrected for Lorentz and polarization effects. Scattering factors for neutral atoms and anomalous dispersion corrections for Cu, Ge, and Nd were taken from the "International Tables for X-Ray Crystallography" (5). The structure was solved by Multan and Fourier methods in two space groups, $C2/m$ and Cm. In fact, most of the atoms occupied centrosymmetric positions, with the exception of two oxygens, O(5) and O(10), which broke the centrosymmetric $C2/m$ group. Because of this the acentric Cm group was chosen. An empirical absorption correction (6) was applied at the end of the isotropic refinements. Mixed full-matrix least-squares refinements minimizing $\sum w(|F_o| - |F_c|)^2$ with weights $w = w_1w_2$, where $w_1 = 1/(a + b|F_o|)^2$ and $w_2 = 1/[c + d(\sin\theta/\lambda)]$ and coefficients given in Table 2, led to the R value of 0.051. Final difference synthesis showed no significant electron density. Most of the calculations were carried out with the X-ray 76 system (7).

TABLE 1
Crystal and Refinement Data

Formula	$CuNd_2Ge_2O_8$
Formula wt	*625.2*
Crystal system	monoclinic
Space group	*Cm* (No. 8)
Cell dimensions	
a, Å	9.846(2)
b, Å	15.335(5)
c, Å	8.336(1)
β, °	148.48(2)
Z	4
V, Å^3	657.9(5)
D_{calcd}, g cm^{-3}	6.31
F(000)	1108
Temp, °C	22
Diffractometer	Enraf-Nonius
Radiation	graphite-monochromated Mo$K\alpha$ (λ = 0.71069 Å)
μ(Mo$K\alpha$), cm^{-1}	277
Crystal dimensions, mm	0.2 × 0.1 × 0.05
θ range, °	1–30
Scan technique	$\omega/2\theta$
Scan speed range, ° cm^{-1}	0.98–16.48
Data collected	(−13, 0, 0) to (13, 21, 11)
Unique data	997
Observed reflections $I > 2\sigma(I)$	946
Decay	≤1%
R_{int}, %	4.9
Standard reflections	3/90
$R = \sum \|\Delta F\|/\sum \|F_o\|$	5.1
$R_w = (\sum w \Delta^2 F/\sum w \|F_o\|^2)^{1/2}$	5.7
Average shift/error	0.03
Absorption correction range	1.55–0.77

TABLE 2
Coefficients for the Weighting Scheme

	a	*b*	*c*	*d*
$\|F_o\| < 40$	7.42	−0.11		
$40 < \|F_o\| < 590$	1.24	0.04		
Sin $\theta/\lambda < 0.41$			6.23	−13.27
$0.4 <$ Sin $\theta/\lambda < 0.71$			0.53	0.25

TABLE 3
Atomic Parameters for $CuNd_2Ge_2O_8$

Atom	x/a	y/b	z/c	U_{eq}[a]
Nd1	0.4700(0)	0.1205(0)	0.2300(0)	6(1)
Nd2	0.4616(3)	0.1198(0)	0.7181(3)	6(1)
Ge1	0.4185(8)	0.5000(0)	0.4235(10)	4(4)
Ge2	0.5090(9)	0.5000(0)	1.0106(11)	5(3)
Ge3	0.4791(5)	0.2904(1)	0.4970(7)	7(2)
Cu1	0.4761(5)	0.2929(2)	0.9482(7)	10(3)
O1	0.2131(35)	0.5000(0)	0.0472(43)	6(3)
O2	0.2166(37)	0.0000(0)	0.3852(46)	9(3)
O3	0.2236(36)	0.0000(0)	0.0613(43)	7(3)
O4	0.2114(38)	0.5000(0)	0.3806(46)	10(3)
O5	0.1304(26)	0.0928(9)	0.6342(31)	10(3)
O6	0.1532(24)	0.3269(8)	0.1576(30)	8(2)
O7	0.3078(26)	0.4072(9)	0.8044(30)	9(2)
O8	0.3222(23)	0.1731(8)	0.3318(28)	6(2)
O9	0.1799(22)	0.2405(8)	0.5303(26)	8(2)
O10	0.1550(23)	0.2336(8)	0.8479(27)	10(2)

[a] $U_{eq} = 1/3 \sum_i \sum_j U_{ij} a_i^* a_j^* \mathbf{a}_i \cdot \mathbf{a}_j \cdot 10^3$

III. RESULTS

$CuNd_2Ge_2O_8$ crystals had sizes of up to 3 mm and appeared as elongated prisms bounded by a pinacoidal face. All of them were blue, refringent, and showed a vitreous brilliance. Their unit-cell dimensions are given in Table 1. Atomic position coordinates and thermal parameters, as well as main interatomic distances and angles, are included in Tables 3 and 4.

Ge atoms in $CuNd_2Ge_2O_8$ exhibit two different coordination polyhedra. Both Ge(1) and Ge(2) show the usual tetrahedral coordination, with distances and angles quite similar to those found (8, 9) in $CuGeO_3$ and $Ge_6O_{12}\cdot NMe_4OH$. On the other hand, Ge(3) atoms form GeO_5 trigonal bipyramids with two apical oxygens at average distances of 1.95 Å, longer than the average of the three equatorial ones, 1.77 Å, and in the same manner of the GeO_2 inclusion compound mentioned (9) in which these average distances are 1.91 and 1.78 Å. Cu atoms form CuO_6 octahedra which are elongated but not to such an extent as those present (8) in $CuGeO_3$ since Cu–O apical distances in $CuNd_2Ge_2O_8$ are 2.65(3) and 2.55(3) Å against 2.77 Å in $CuGeO_3$. CuO_6 octahedra are very deformed because they show not only a very large Jahn–Teller distortion and a rhomboidal equatorial plane, but also different distances from Cu to the apical oxygens and an O(10)–Cu–O(10′) angle of 144.7(1)°.

Nd(1) and Nd(2) atoms coordinate to eight oxygens giving rise to similar NdO_8 polyhedra. As can be seen in Fig. 1, both are situated between two almost parallel planes, P1 and P2, of which P1 is formed by [O(8), O(7), O(5), O(4)] for Nd(1) and by [O(9), O(6), O(8), O(7)] for Nd(2); P2 is formed by [O(9), O(6), O(10)] for Nd(1) and by [O(5), O(2), O(1)] for Nd(2). In both cases the eighth oxygen is outside of the planes, in such a way that the eighth Nd–O direction is nearly perpendicular to both planes. It can be concluded that the NdO_8 polyhedra are triangulated dodecahedra, one of the most stable for octacoordination. The results of the planarity study around Nd atoms are shown in Table 5.

The structure of $CuNd_2Ge_2O_8$ can be described as containing chains of CuO_6 octahedra which share O(10) apical vertices in the *a* direction. Chains of CuO_6 octahedra are linked in the *b* direction through $Ge(2)O_4$ tetrahedra with which they share vertices forming layers like those represented in Fig. 2. These alternate with other layers like those of Fig. 3, formed by the association $Ge(3)O_5$–$Ge(1)O_4$–$Ge(3)O_5$, consisting of two GeO_5 triangular bipyramids and one GeO_4 tetrahedron which share vertices in the *b* direction. Layers of both kinds are mutually connected in the *c* direction (Fig. 4) through the $Ge(3)O_5$ bipyramids that have one common face with the CuO_6

TABLE 4
Interatomic Distances (Å) and Angles (°)

Nd1–O3	2.34	Nd2–O1	2.33
Nd1–O4	2.35	Nd2–O2	2.34
Nd1–O5	2.78	Nd2–O5	2.72
Nd1–O6	2.47	Nd2–O6	2.42
Nd1–O7	2.65	Nd2–O7	2.85
Nd1–O8	2.37	Nd2–O8	2.32
Nd1–O9	2.50	Nd2–O9	2.48
Nd1–O10	2.43	Nd2–O10	2.52
Ge1–O1	1.76	Ge2–O2	1.75
Ge1–O4	1.74	Ge2–O3	1.77
Ge1–O5	1.79 × 2	Ge2–O7	1.76 × 2
Ge3–O5	1.96	Cu–O6	2.07
Ge3–O6	1.77	Cu–O7	1.97
Ge3–O8	1.97	Cu–O8	1.88
Ge3–O9	1.81	Cu–O9	1.99
Ge3–O10	1.75	Cu–O10	2.65
Cu–O10′	2.55		
O1–Ge1–O4	105.5	O2–Ge2–O3	103.5
O1–Ge1–O5	110.7 × 2	O2–Ge2–O7	112.0 × 2
O4–Ge1–O5	112.5 × 2	O3–Ge2–O7	110.7 × 2
O5–Ge1–O5	105.0	O7–Ge2–O7	107.9
O5–Ge3–O6	94.8	O6–Ge3–O9	125.6
O5–Ge3–O8	174.5	O6–Ge3–O10	127.0
O5–Ge3–O9	87.8	O8–Ge3–O9	88.4
O5–Ge3–O10	92.3	O8–Ge3–O10	92.6
O6–Ge3–O8	84.2	O9–Ge3–O10	107.1
O6–Cu–O7	166.6	O7–Cu–O10	113.6
O6–Cu–O8	79.0	O7–Cu–O10′	87.4
O6–Cu–O9	92.4	O8–Cu–O10	81.1
O7–Cu–O8	98.8	O8–Cu–O10′	125.3
O7–Cu–O9	94.4	O9–Cu–O10	74.6
O8–Cu–O9	156.3	O9–Cu–O10	75.6
O6–Cu–O10	79.3	O10–Cu–O10′	144.7
O6–Cu–O10′	83.2		

Note. Average e.s.d.'s 0.02 (Å) and 0.9 (°).

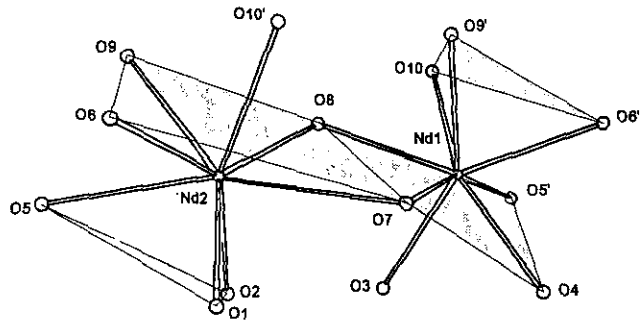

FIG. 1. NdO_8 coordination polyhedra in $CuNd_2Ge_2O_8$. Shadowed areas correspond to the calculated planes given in Table 5.

octahedra giving rise to the mentioned deformation. In this way a 3D structure results as Fig. 5 illustrates. Nd(1)O_8 and Nd(2)O_8 polyhedra occupy rather large holes of the whole structure.

In $CuNd_2Ge_2O_8$ every four NdO_8 dodecahedra are associated by sharing edges forming tetrameric units (Fig. 6). From the point of view of the NdO_8-polyhedra packing, the resulting structure can be conceived as an alternate association of these tetrameric units which share vertices and edges in the *c* and *a* directions, respectively. This sort of packing gives rise to three different kind of interstices: tetrahedra at the center of each unit, in which Ge(1) and Ge(2) are lying, and octahedra and trigonal bipyramids, formed in the unions between different units which are occupied by Cu and Ge(3) atoms, respectively.

The reciprocal dc magnetic susceptibility of $CuNd_2Ge_2O_8$ follows a Curie–Weiss law above nearly 100 K, $\chi^{-1} = 162(1)T + 5971(93)$ g Oe/emu, with a Weiss constant of $\theta = 36.8(7)$ K and a correlation factor $R = 0.99997$ (Fig. 7). From the magnetization value at room temperature and considering Nd^{3+} as the only contributing ion, a magnetic moment of 3.72(9) μ_B per atom is obtained. But if the effective moment for Nd^{3+} is assumed to be that observed in the absence of interactions, 3.5 μ_B, another magnetic species with 1.78(7) μ_B must be included. This could be the Cu^{2+} cation, although its free-ion moment is a little

TABLE 5
Angles (°) between Principal Planes and Lines in NdO_8 Polyhedra

	Nd 1	Nd 2
P1	O7–O8–O5′–O4	O7–O8–O9–O6
P2	O10–O9′–O6′	O2–O5–O1
L	Nd1–O3	Nd2–O10′

P1(Nd1) ∧ P2(Nd1)	156.4(5)
P1(Nd2) ∧ P2(Nd2)	161.3(7)
P1(Nd1) ∧ P1(Nd2)	167.8(4)
P1(Nd1) ∧ P2(Nd2)	165.3(7)
P2(Nd1) ∧ P2(Nd2)	154.1(5)
P2(Nd1) ∧ P2(Nd2)	171.1(7)
P1(Nd1) ∧ L(Nd1)	86.4(4)
P1(Nd2) ∧ L(Nd2)	72.6(6)
L(Nd1) ∧ L(Nd2)	169.0(8)

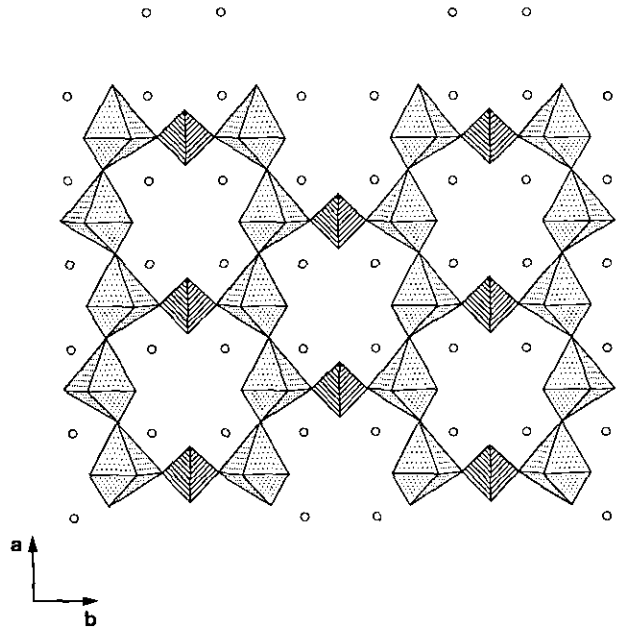

FIG. 2. Layers formed in the *b* direction of $CuNd_2Ge_2O_8$ by chains of CuO_6 octahedra linked by common vertices of GeO_4 tetrahedra.

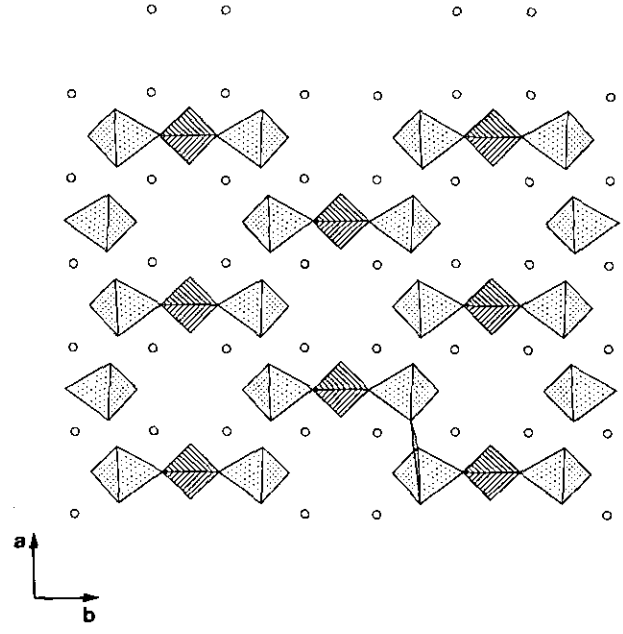

FIG. 3. Layers resulting in $CuNd_2Ge_2O_8$ from the association in the *b* direction of two GeO_5 trigonal bipyraids and one GeO_4 tetrahedron through common vertices.

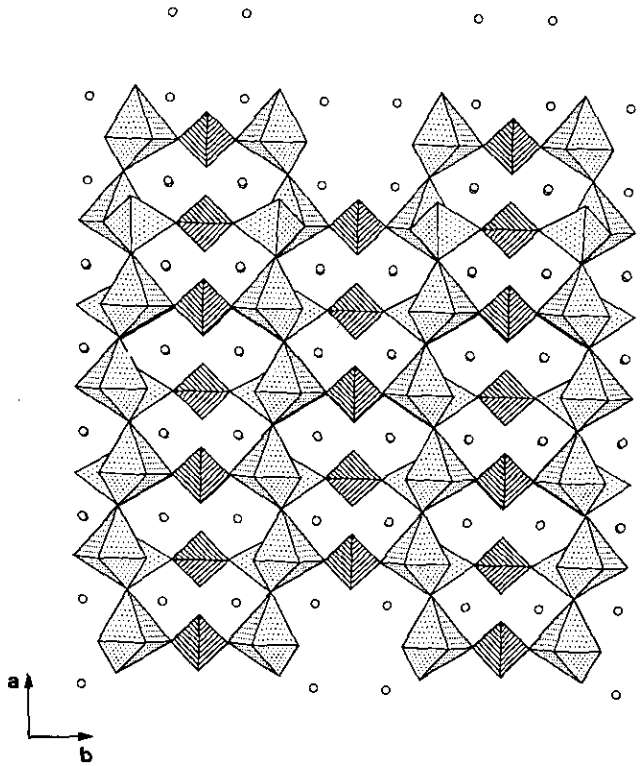

FIG. 4. Projection in the *ab* plane of alternating layers of $CuNd_2Ge_2O_8$ like those of Figs. 2 and 3.

bit smaller than that measured, 1.9 μ_B. Effectively, the measurements performed in $CuY_2Ge_2O_8$ that contains Cu^{2+} as the only magnetic cation lead to a correlation factor of 0.9992 and to 1.80 μ_B at 296 K. On the other hand, the deviation from linearity observed at low temperature in the inverse susceptibility vs T plot (Fig. 7) could be related to a magnetic coupling between Cu and Nd moments, although more frequently it is attributed (10) to the splitting of the free-ion ground state under the influence of the crystal field. The Weiss constant could be then entirely

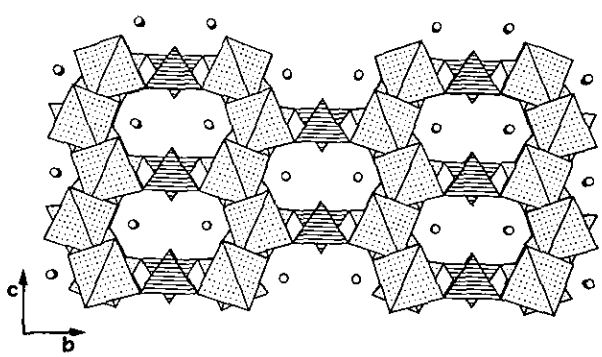

FIG. 5. Layers in $CuNd_2Ge_2O_8$ like those of Figs. 2 and 3 connected in the *c* direction by GeO_5 bipyramids that have one common face with CuO_6 octahedra. Projection in the *cb* plane.

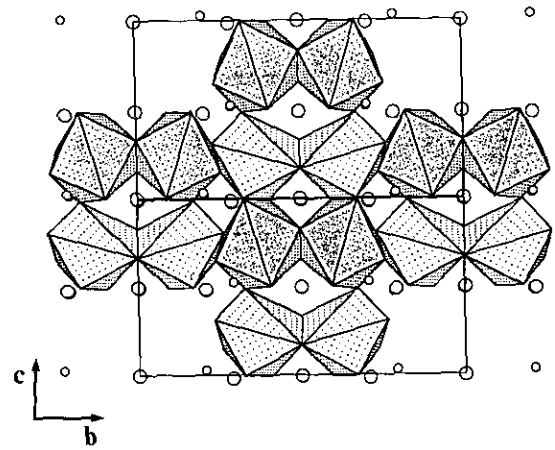

FIG. 6. Association of tetrameric $(NdO_8)_4$ units in $CuNd_2Ge_2O_8$. Small circles represent Cu ions and large circles Ge atoms. $Nd(1)O_8$ and $Nd(2)O_8$ are shown by white and shadowed polyhedra, respectively.

due to the crystal field. Such deviation is also present in CuY_2GeO_8, favoring, therefore, the second hypothesis.

The characteristic IR absorptions are shown in Fig. 8. It is not possible to make even an approximate assignment of these very complex spectra, but it is evident that most of the bands in the spectral range 800–400 cm^{-1} are related to vibrations of the GeO_4 and GeO_5 groups. This supposition is reinforced by the fact that recently in some novel GeO_2 inclusion compounds (9, 11), and especially in those better characterized like $Ge_6O_{12} \cdot NMe_4OH$, whose framework consists of GeO_4 tetrahedra and GeO_5 trigonal bipyramids, the observed absorption bands at 837 and 567/521 cm^{-1} were assigned to the Ge–O–Ge stretching vibrations; the former to the asymmetrical stretching and the latter to the symmetrical. The shoulder band found (12) at 790 cm^{-1} when Ge was introduced in the spinel lithium ferrite

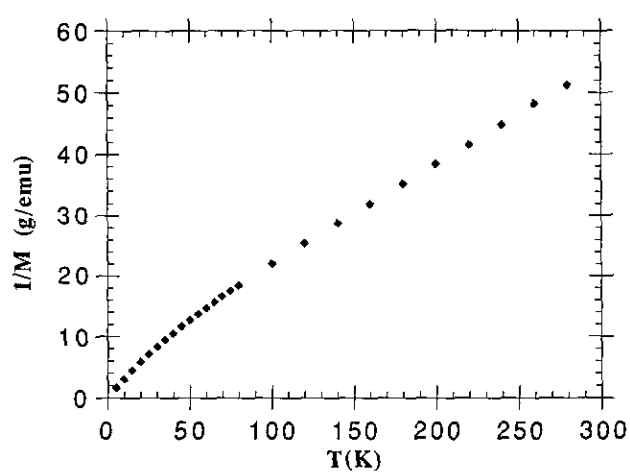

FIG. 7. Reciprocal of the dc magnetic susceptibility of $CuNd_2Ge_2O_8$ as a function of the temperature.

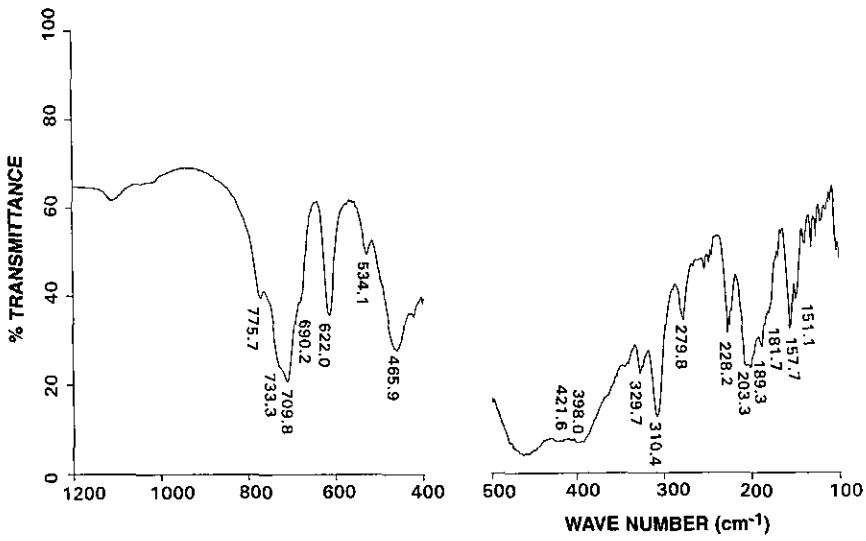

FIG. 8. Infrared spectrum of $CuNd_2Ge_2O_8$.

can be related in the same way to the stretching vibrational modes of GeO_4 tetrahedra. On the other hand, in tetrahedral GeF_4 the observed (13) bands at 795 and 270 cm^{-1} are assigned to the active modes ν_3 and ν_4, in agreement with literature spectra (14). However, to our knowledge, the IR vibrations of a trigonal-bipyramidal GeO_5 network has never been reported. Only a few IR studies concerning the similar GeF_5^- anions are known (15). The three bands at 679, 696, and 730 cm^{-1} are assigned (14) to Ge–F stretching vibrations, because, although a strict D_{3h} geometry will give rise to only two IR-active Ge–F stretching modes, probably an effective lower symmetry for GeF_5^- is present. A good number of the remaining vibrations correspond probably not only to the Nd–O bond stretching coordinates (16, 17), but also to the Cu-polyhedra stretching, as indicated (18) for a series of mixed rare-earth copper oxides, $CuNdRO_4$ (R = La, Nd, Sm, Gd, Dy). Finally, the lower wavenumbers, below 300 cm^{-1}, can be due to the remaining bending and more complex vibrations of the different bonds present in $CuNd_2Ge_2O_8$.

Although the absorption spectrum in the region 350–700 nm was taken at room temperature, where all the Stark components of the $^4I_{9/2}$ ground state manifold for both $Nd(1)^{3+}$ and $Nd(2)^{3+}$ are thermally populated, the recorded spectrum shows the characteristic groups of transitions for a Nd-containing matrix, the more intense being $^4I_{9/2} \rightarrow {}^2P_{1/2}$ (430–439 nm); $^4I_{9/2} \rightarrow {}^4G_{9/2}$, $^2K_{13/2}$, $^4G_{7/2}$ (512–542 nm); and $^4I_{9/2} \rightarrow {}^4G_{5/2}$, $^4G_{7/2}$, $^2G_{7/2}$ (571–608 nm). In order to establish a complete energy-level scheme for both Nd^{3+} in that structure and to determine the phenomenological crystal-field parameter sets, a careful study of the absorption spectra at liquid-helium temperature has been now undertaken.

ACKNOWLEDGMENTS

This work was supported by the Comisión Interministerial de Ciencia y Tecnología, under Project PB94-0031. The helpful comments of P. Porcher and J. Marco are acknowledged.

REFERENCES

1. J. A. Campá, E. Gutiérrez-Puebla, M. A. Monge, I. Rasines, and C. Ruíz Valero, *J. Cryst. Growth* **125,** 17 (1992).
2. Powder Diffraction File, Card No. 34-384. International Centre for Diffraction Data, Swarthmore, PA.
3. U. Lambert and W. Eysel, *Powder Diffr.* **1,** 256 (1986).
4. Ch.J. O'Connor, *in* "Progress in Inorganic Chemistry" (S. J. Lippard, Ed.), Vol. 29, p. 210. Wiley, New York, 1982.
5. J. A. Ibers and W. C. Hamilton, Eds., "International Tables for X-Ray Crystallography." Vol. IV, p. 79, 80, and 88. Kynoch, Birmingham, England, 1974.
6. N. Walker and D. Stuart, *Acta Crystallogr. Sect. A* **39,** 158 (1983).
7. J. M. Stewart, P. A. Machin, C. W. Dickinson H. L. Ammon, H. Heck, and H. Flack, "The X-Ray 76 System." Technical Report TR-446, Computer Science Center, Univ. of Maryland, College Park, MD, 1976.
8. H. Völlenkle, A. Wittmann, and H. Nowotny, *Monatsh. Chem.* **98,** 1352 (1967).
9. J.Cheng, R. Xu, and G. Yang, *J. Chem. Soc. Dalton Trans.* 1537 (1991).
10. C. Cascales, R. Sáez-Puche, and P. Porcher, *J. Solid State Chem.* **114,** 52 (1995).
11. J. Cheng and R. Xu, *J. Chem. Soc., Chem. Commun.* 483 (1991).
12. S. A. Mazen, M. H. Abdallah, R. I. Nakhla, and H. M. Zaki, *Mater. Chem. Phys.* **34,** 35 (1993).
13. A. M. McNair and B. S. Ault, *Inorg. Chem.* **21,** 1762 (1982).
14. F. Koninger, A. Muller, and W. Orville-Thomas, *J. Mol. Struct.* **37,** 199 (1977).
15. A. M. McNair and B. S. Ault, *Inorg. Chem.* **21,** 2603 (1982).
16. I. L. Botto, E. J. Baran, C. Cascales, I. Rasines, and R. Sáez Puche, *J. Phys. Chem. Solids* **52,** 431 (1991).
17. B. F. Dzhurinskii, I. V. Tananaev, E. G. Tselebrovskaya, and A. I. Prozorovskii, *Izv. Akad. Nauk SSSR, Neorg. Mater.* **27,** 255 (1991).
18. V. B. Lazarev, I. S. Shaplygin, *Russ. J. Inorg. Chem.* **26,** 947 (1981).